Research Article

# Reconstructing Phreatic Palaeogroundwater Levels in a Geoarchaeological Context: A Case Study in Flanders, Belgium

Ann Zwertvaegher,[1,*] Peter Finke,[1] Jeroen De Reu,[2] Alexander Vandenbohede,[1] Luc Lebbe,[1] Machteld Bats,[2] Wim De Clercq,[2] Philippe De Smedt,[4] Vanessa Gelorini,[1] Joris Sergant,[2] Marc Antrop,[3] Jean Bourgeois,[2] Philippe De Maeyer,[3] Marc Van Meirvenne,[4] Jacques Verniers,[1] and Philippe Crombé[2]

[1]Department of Geology and Soil Science, Ghent University, Ghent, Belgium
[2]Department of Archaeology, Ghent University, Ghent, Belgium
[3]Department of Geography, Ghent University, Ghent, Belgium
[4]Department of Soil Management, Ghent University, Ghent, Belgium

**Correspondence**
*Corresponding author;
E-mail: Ann.Zwertvaegher@ugent.be

**Received**
12 March 2012
**Accepted**
10 December 2012

Scientific editing by Jamie Woodward

Published online in Wiley Online Library (wileyonlinelibrary.com).

doi 10.1002/gea.21435

The complex debate on prehistoric settlement decisions is no longer tackled from a purely archaeological perspective but from a more landscape-oriented manner combined with archaeological evidence. Therefore, reconstruction of several components of the former landscape is needed. Here, we focus on the reconstruction of the groundwater table based on modeling. The depth of the phreatic aquifer influences, for example, soil formation processes and vegetation type. Furthermore, it directly influences settlement by the wetness of a site. Palaeogroundwater modeling of the phreatic aquifer was carried out to produce a series of full-coverage maps of the mean water table depth between 12.7 ka and the middle of the 20th century (1953) in Flanders, Belgium. The research focuses on the reconstruction of the input data and boundary conditions of the model and the model calibration. The model was calibrated for the 1924–1953 time period using drainage class maps. Archaeological site data and podzol occurrence data act as proxies for local drainage conditions over periods in the past. They also served as a control on the simulated phreatic palaeogroundwater levels. Model quality testing on an independent validation data set showed that the model predicts phreatic water table levels at the time of soil mapping well (mean error of 1.8 cm; root mean square error of 65.6 cm). Simulated hydrological conditions were in agreement with the occurrence of archaeological sites of Mesolithic to Roman age at 96% of the validation locations, and also with the occurrence of well-drained podzols at 97% of the validation locations. © 2013 Wiley Periodicals, Inc.

## INTRODUCTION

It is generally agreed that the human occupation of a region in pre- and protohistoric times was influenced by the landscape, as well as by motivations of a more political, socioeconomic, and cultural nature (Thomas, 1993; Tilley, 1994; Jordan, 2001; Kamermans, 2006; Zvelebil, 2003). In this light, a more landscape-oriented point of view is often taken, examining the archaeological evidence in its spatial setting. Often however, the current state of some landscape components deviates from their pre- and protohistoric state. Therefore, reconstructions of the palaeolandscape are needed. Several examples are found in the literature, focusing on the reconstruction of different landscape components such as hydrology (Gyucha, Duffy, & Frolking, 2011), vegetation (Spikins, 1999, 2000), and topography (Oregon & Fiz, 2008).

The area of interest is situated in the Flanders region in northern Belgium, an area dominated by sandy soils and known as Sandy Flanders. In recent decades the region has been subject to extensive and systematic field research, revealing areas rich and poor in archaeological evidence. Despite repeated archaeological surveys, the latter areas revealed little or no archaeological material (Sergant, Crombé, & Perdaen, 2009; Crombé et al., 2011). To find the possible reasons for this apparently

 Copyright © 2013 Wiley Periodicals, Inc.

discontinuous population and exploitation of the region, an interdisciplinary and landscape-oriented approach was developed. A land evaluation based on reconstructed components of the palaeolandscape was proposed (Zwertvaegher et al., 2010). In this evaluation, the suitability of the land for a specific land use is evaluated based on land qualities. Zwertvaegher et al. (2010) list various biophysical attractors for occupation (such as suitable places for hunting, fishing, gathering, settlement, and agriculture) that are associated with land qualities that relate to vegetation, soil, elevation, river network hydrology, as well as water table depth. For example, rainfed agricultural potential is influenced by moisture and oxygen availability in the soil, which in turn is dependent on the depth of the groundwater table. Settlement is largely determined by the wetness of a site, which is also affected by the water table depth. Because geoarchaeological data are often limited spatially and temporally, process models can be used to reconstruct the former state(s) of these landscape components. Such process models mimic the behavior of a system using equations or decision rules built on knowledge of natural processes (Zwertvaegher et al., 2010). Furthermore, the simulated values from one process model can serve as inputs for another process model.

The overall objective of this study is to attempt a reconstruction of the phreatic palaeogroundwater levels for the defined study area in Sandy Flanders since the end of the Late Glacial—encompassing a total of 12,720 years—by the use of a groundwater flow model. This requires the reconstruction of boundary conditions, such as climate and vegetation, hydrological network and topography. The model is calibrated for the period 1924–1953 with full-coverage observations derived from a soil map. Furthermore, we propose the use of archaeological and podzol evidence as proxies for local drainage conditions over periods in the past, serving as a plausibility check on the simulated phreatic palaeogroundwater levels.

## STUDY AREA AND PERIOD

### Geological Context

The study area (584 km$^2$) is located in Flanders, in the northern part of Belgium (Figure 1A). During the Pleistocene (Figure 2 for all chronostratigraphical and archaeological periods), large river systems primarily draining to the north and later to the northwest, formed the paleovalley called the Flemish Valley (De Moor & Heyse, 1978; Figure 1B). Valley filling by braided river systems during the Pleniglacial resulted in a smoothed surface with typical microrelief (De Moor & Heyse, 1978). The mainly sandy infillings reach thicknesses up to 20 m (Jacobs et al., 1993). Aeolian activity in the region increased, reworking the exposed fluvial sediments and creating parallel east–west oriented dunes and dune complexes (De Moor & Heyse, 1974; Heyse, 1979). The most pronounced of these dune complexes accumulated between Maldegem in the west and Stekene in the east, which gradually lead to the damming of the northwestward braided river system, forcing the drainage toward the east, and the creation of numerous shallow lakes along its southern edge (De Moor & Heyse, 1978; De Moor & van de Velde, 1995). The Moervaart palaeolake (Figure 1B) was the largest one within Sandy Flanders, covering *ca.* 25 km$^2$ (Crombé et al., 2012). At the transition from the Allerød to the Younger Dryas the drainage network changed, with the disappearance of the Moervaart palaeolake and the appearance of a more meandering drainage pattern with a deeply incised and laterally stable river channel, now called the Kale/Durme. For much of the Holocene the region was geomorphologically quite stable. However, due to the impact of humans this situation changed beginning in the Subatlantic with local sand drifting in the Roman Period (Verbruggen, 1971) and peat cutting in Medieval times (Jongepier et al., 2011).

### Archaeological Context

The Late Glacial human occupation in the study region started in the Allerød with Final Palaolithic *Federmesser* groups occupying the entire area, but with a clear preference for the northern bank of the Late Glacial Moervaart lake (Figure 1C; Crombé & Verbruggen, 2002; Van Vlaenderen et al., 2006; Crombé et al., 2011). During the Early Mesolithic the distribution of sites appeared to be very similar to *Federmesser* times (Crombé et al., 2011). However, as the large Moervaart lake had already disappeared completely, the occupation now preferentially concentrated along the margins of Kale/Durme river channels. During the Middle and Late Mesolithic, the site density decreased, site complexes no longer occurred, and campsites were more widely spaced. However, riverbanks remained the most favored settlement location (Crombé et al., 2011). In the Late Mesolithic, sites appeared to be located on lower-lying land and less reoccupation of former campsites occurred (Crombé et al., 2011). The first Neolithic colonization of Sandy Flanders started around 6.0 ka with semimobile Michelsberg groups, operating in the wetlands, but most likely also in the drier regions of Sandy Flanders (Crombé & Sergant, 2008). Information on the Early and Middle Bronze Age originates mainly from funerary monuments (barrows) (Bourgeois & Cherretté, 2005). Topographical analysis of the Bronze

 Copyright © 2013 Wiley Periodicals, Inc. 

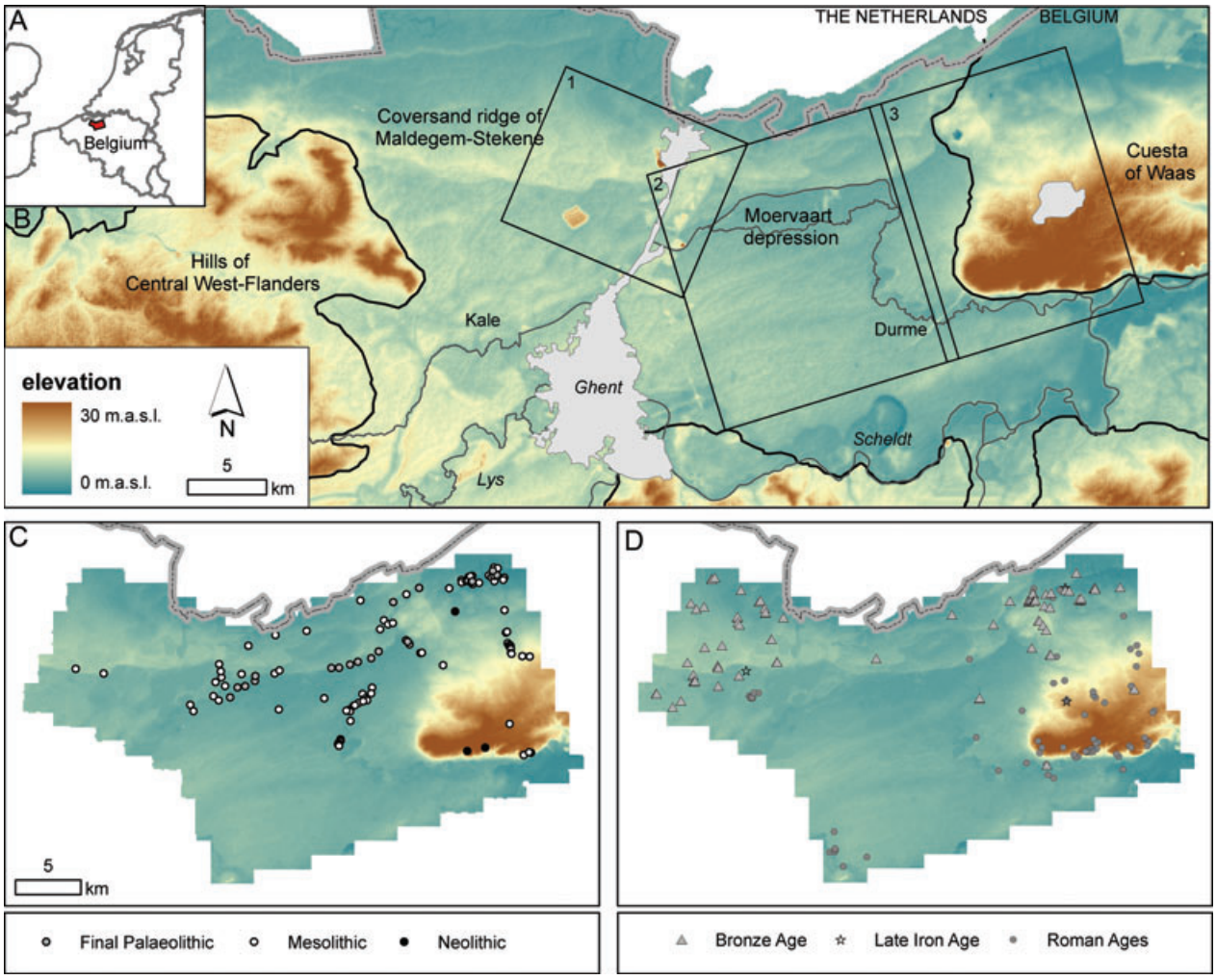


**Figure 1** (A) Location of Belgium with the study area (in red); (B) digital elevation model showing the three partly overlapping subareas of the groundwater model indicated with open squares (subareas 1, 2, and 3), several geomorphological units and the extent of the Flemish Valley (bold black line; based on De Moor & Heyse, 1978); (C) final Palaeolithic Federmesser, Mesolithic and Neolithic find spots (Sergant et al., 2009); (D) Bronze Age barrows (Early and Middle Bronze Age; De Reu et al., 2011a, 2011c) and Late Iron Age and Roman (De Clercq, 2009) sites.

Age barrows showed a clustering of these burial mounds at higher grounds and in prominent locations in the landscape, with a preference for ridges and upslope areas, while in other areas they appear to be totally absent (Figure 1D; De Reu et al., 2011b). Bronze Age settlements, on the other hand, are less well-documented and still poorly understood. A slightly higher density of Late Bronze Age and Early Iron Age settlement sites compared to the earlier Bronze Age periods is found (Bourgeois, Cherretté, & Bourgeois, 2003). During the entire Bronze and Iron Ages, a comparable pattern can be found, with a dense and continuous habitation of the regions in the western and eastern part of the study area, while the more central part apparently showed no sign of habitation (De Reu et al., 2010). The same pattern appears to exist in Roman times (De Clercq, 2009).

## METHODOLOGY

### Available Data Sources

Several sources of information were available for the study region and were used in various steps of the research (Table I). Present-day topographical information was supplied as a high-precision digital elevation model (present DEM), constructed by Werbrouck et al. (2011) from high-density airborne LiDAR data. Furthermore, artifacts caused by modern objects and infrastructure

 Copyright © 2013 Wiley Periodicals, Inc.

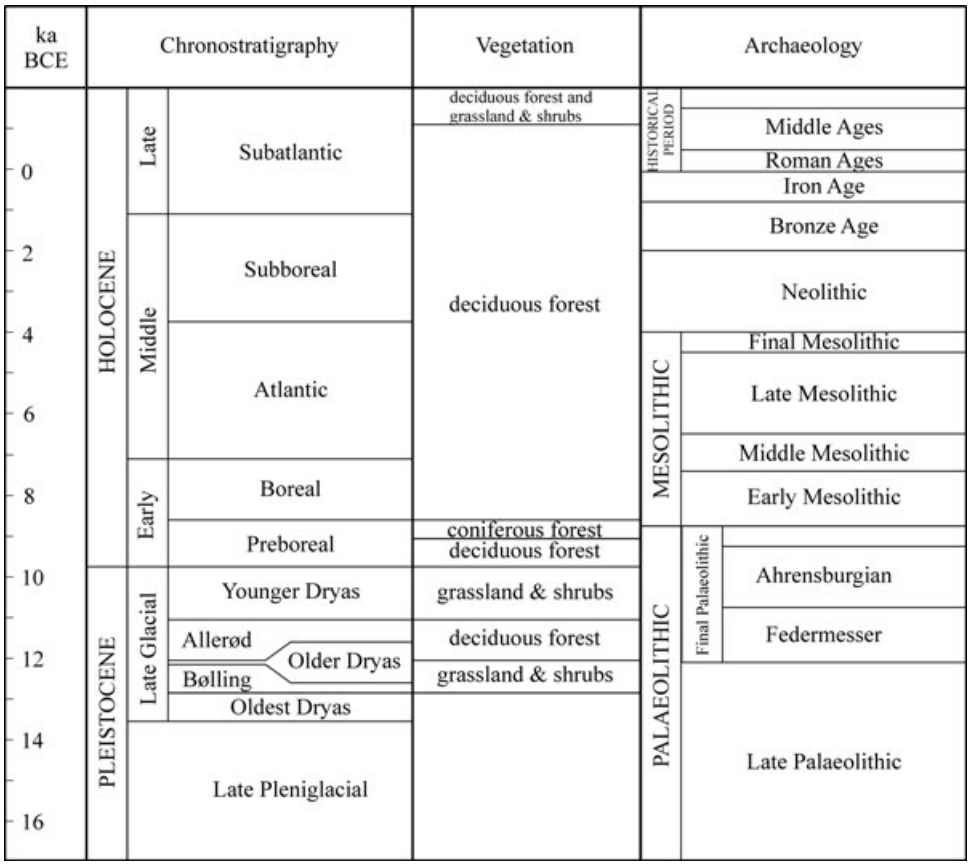


**Figure 2** Timetable listing the chronostratigraphical units and archaeological periods of the last 20 ka. Ages are expressed in ka B.C.E. Chronostratigraphy of the Holocene is based on Terberger, Barton, and Street (2006); the subdivision of the Pleistocene is based on radiocarbon dated pollen diagrams for the Netherlands, as revised by Hoek (2001). The time frame of the archaeological periods is expressed for the situation in Sandy Flanders. Note that at present, no traces of the Late Palaeolithic and Ahrensburgian cultures have been reported in Sandy Flanders (Crombé & Verbruggen, 2002; Crombé et al., 2011). The vegetation type as applied in the model is also indicated.

created since the 19th century were removed providing a DEM that was useful for historical geographical purposes (Werbrouck et al., 2011; post-medieval DEM). Information on soil texture class, drainage class, and soil profile was recorded in the soil map (sampling density of two observations per hectare). During a soil survey campaign, thousands of profiles were analyzed and collected in the Aardewerk database (Van Orshoven et al., 1988). A more recent mapping of the drainage classes was performed by measurements of the water table in a small part of the study area (Zidan, 2008). Furthermore, the region is rich in historical maps dating between the 16th and 19th centuries. Eighty historical maps of the study area, covering a large range of spatial extents and scales, were collected and scanned by the Department of Geography of Ghent University. Based the on well-documented historical maps produced by Ferraris, Vandermaelen, and the third edition topographical maps, De Keersmaeker et al. (2001) constructed forest distribution maps for the years 1775, 1850, and 1930. Furthermore, colored orthophotographs, Quaternary geological and hydrogeological maps were available for the full extent of the study area.

Vector data on the location and classification of the present-day watercourses of Flanders were obtained from the Flemish Hydrographical Atlas (FHA). Archaeological data covering the study period were provided by the Department of Archaeology of Ghent University. Considering the study period, these concerned sites and/or find spots from the Mesolithic and Neolithic (Sergant, Crombé, & Perdaen, et al., 2009), Bronze Age barrows (De Reu et al., 2011a, 2011c), and Late Iron Age and Roman sites (De Clercq, 2009). Daily precipitation and evapotranspiration data in a 30-year time series (for the

 Copyright © 2013 Wiley Periodicals, Inc. 

**Table I** Data used in the phreatic groundwater modeling and associated spatial and temporal resolution and typical errors or confidence levels.

| Data set | Source | Date | Data type | Resolution | | Primary interest | Typical error or confidence |
|---|---|---|---|---|---|---|---|
| | | | | Spatial | Temp. | | |
| Present DEM | Werbrouck et al. (2011) | 2001–2004 | Raster | 2 m × 2 m | Table III | Topography | <5 cm |
| Post-medieval DEM | Werbrouck et al. (2011) | - | Raster | 2 m × 2 m | Table III | Topography | <10 cm |
| (Pre)historic DEM | - | - | Raster | 2 m × 2 m | Table III | Topography; hydrology | <20 cm |
| Colored orthophotographs | AGIV | 2002 | Raster | 1:12,000 | NR | Hydrology | HC |
| Soil map | AGIV | 1949–1954 | Raster | 1:20,000 | NR | Topography; calibr. and valid. | 70% purity |
| Hydrogeological maps | DOV | 2002–2006 | Raster | 100 m × 100 m | NR | Hydrogeology | Unknown |
| Drainage class map | Zidan (2008) | 2008–2009 | Raster | 5 m × 5 m | 30 year | Calibr. and valid. | 61% purity |
| Historical maps | Ghent Univ. | 1569–1870 | Raster | Varying | NR | Hydrology | Unknown |
| Forest distribution maps | De Keersmaeker et al. (2001) | 1771–1778; 1846–1854; 1920–1940 | Raster | 1:20,000 | Table III | Vegetation; recharge | HC |
| Flemish Hydrographical Atlas (FHA) | AGIV | 1991–2010 | Vector | 1:50,000 | NR | Hydrology | HC |
| Quaternary map | AGIV | 1993–1999 | Vector | 1:10,000 | NR | Topography | Unknown |
| Archaeological data | Ghent Univ. | 1980–ongoing | Vector | - | - | Calibr. and valid. | HC |
| Meteorological data | Royal Meteorological Institute Belgium | 1977–2006 | Time series | - | 1 day | Climate; recharge | <1 mm $day^{-1}$ |
| Precipitation and temperature anomalies for central western Europe | Davis et al. (2003; personal communication, 2008) | 12,000 B.C.E.–1950 C.E. | Time series | - | 100 year | Climate; recharge | <50 mm $y^{-1}$ <2°C |
| Aardewerk database | Van Orshoven et al. (1988) | 1950–1953, 1963 | Numerical point data | NR | NR | Topography; calibr. and valid. | <10 cm |

HC means high confidence, NR is not relevant.

period 1977–2006; from the Merendree-Schipdonk and Melle weather stations), a 1-year daily temperature series (for 2005 from Uccle weather station), as well as precipitation and temperature anomalies (from 12 ka to the middle of the last century (1950)) for central western Europe, provided by Davis et al. (2003; personal communication, 2008), were also used.

## Model Description

The groundwater heads were calculated using MODFLOW, the three-dimensional USGS groundwater model code (Harbaugh & McDonald, 1996) and known as the worldwide standard groundwater flow model, as evidenced by its application in a wide variety of groundwater studies (e.g., Wilsnack et al., 2001; Zhang & Hiscock, 2010; Zume & Tarhule, 2011). For computational reasons, the study area with a spatial extent of 584 $km^2$ was divided into three subareas (Figure 2), whose orientation and location was defined by the general direction of the groundwater streamlines and by large hydrological differences related to geomorphologic features in the landscape. The grid resolution was set at 100 m × 100 m. The temporal extent of the simulations was 12,720 years, starting at the end of the Late Glacial and covering the Holocene (i.e., 12.7 ka to 1953 C.E.). Note that the soil survey in the study area ended in 1953 so this year was taken as the final year in the simulations. One time step in the simulations represents 30 years. The start date was arbitrarily chosen in the final part of the Younger Dryas. This had to be a product of 30 years because the last time step needed to coincide with 1924–1953. Because the start year and the end year of the simulation are fixed, this sums to a total of 12,720 years.

 Copyright © 2013 Wiley Periodicals, Inc.

Based on the large temporal extent, simulations were performed in the steady-state mode of MODFLOW, having a temporal resolution of 30 years (i.e., a climatic period as defined by Finke et al., 2004). This resulted in maps of the mean water table (MWT) for a total of 424 simulation periods. The final results, provided as MWT depths below the surface, were constructed by subtracting the model output values, expressed in absolute heights, from the topography. Because topography in the study area varied during the simulated time period, several temporal DEMs were used and reconstructed when not available as an original data source.

Ranges of values for hydraulic characteristics of the different geological layers in the area are presented in Table II. The depth of their base was derived from the hydrogeological maps, as provided by the Flemish Subsoil Database (DOV). Information on these layers was conceptualized as input to the groundwater model: the vertical discretization was set at 15 computational layers of 5 m thickness and for each computation layer transmissivity, proportional to the horizontal hydraulic conductivity, and vertical hydraulic conductance divided by the layer thickness, was calculated. Model boundary conditions, such as the influence of the local hydrological network and the recharge to the groundwater table per simulation period, were reconstructed and supplied to the model via the MODFLOW packages. Furthermore, in accordance with the Dutch nutrient emission model STONE (Kroon et al., 2001), the drainage of the upper 0.20 m of the soil was also taken into account. This is especially relevant in regions with shallow groundwater levels. Therefore, a uniform hydraulic conductance of the upper soil was applied to the entire study area.

Table II Hydrogeology of the study region: variation in lithology, horizontal hydraulic conductivity ($K_h$), and thickness of several layers in the study area (VMM, 2008a, 2008b).

| Hydrogeology | $K_h$ (m d$^{-1}$) | Thickness (m) |
|---|---|---|
| Quaternary Aquifer System | | |
| Pleistocene sediments | 0.01–30 | 0–25 |
| Pleistocene of the Flemish Valley | | |
| Campine Aquifer System | | |
| Peilstocene and Pliocene Aquifer | | |
| Sandy top of Lillo | 5–18 | 0–42 |
| Miocene Aquifer System | | |
| Sand of Kattendijk and/or bottom sand layer of Lillo | 4–20 | 0–35 |
| Boom Aquitard | $10^{-8}$ | 0–80 |
| Oligocene Aquifer System | | |
| Ruisbroek-Berg Aquifer | | |
| Sand of Ruisbroek | 0.03–5 | 0–20 |
| Tongeren Aquitard | | |
| Clay of Watervliet | $10^{-4}$–$10^{-5}$ | 0–20 |
| Under-Oligocene Aquifer System | | |
| Clayey sand of Bassevelde | 1–5 | 0–30 |
| Bartoon Aquitard System | | 0–50 |
| Clay of Onderdijke | $10^{-4}$–$10^{-6}$ | |
| Sand of Buisputten | $10^{-2}$–$10^{-6}$ | |
| Clay of Zomergem | $10^{-5}$–$10^{-6}$ | |
| Sand of Onderdaele | 0.2–1.7 | |
| Clays of Ursel en/of Asse | $10^{-6}$–$10^{-8}$ | |
| Ledo-Paniselian Brusselian Aquifer System | | |
| Wemmel-Lede Auifer | 0.6–3 | 0–30 |
| Sand of Wemmel | | |
| Sand of Lede | | |
| Sand of Brussel | 6 | 0–15 |
| Sediments of the Upper-Paniselian | 3 | 0–45 |
| Sands of Aalter and/or Oedelem | | |
| Sandy clay of Beernem | | |
| Sandy sediments of the Under-Paniselian | 0.8–6.7 | 0–30 |
| Paniselian Aquitard System | | 0–30 |
| Clay of Pittem | 0.01–1 | |
| Clay of Merelbeke | 0.003 | |

## Reconstructing Model Input and Boundary Conditions for the Temporal Extent of the Study Period

### *Topography*

A modified assessment of the topography was applied for three different time periods (Table III): present, post-medieval, and (pre)historic DEM. The latter DEM is an adjustment of the post-medieval DEM, in which plaggen soils and marine and alluvial Scheldt deposits were removed. Plaggen management was generally established in the Middle Ages in large parts of Western Europe (Blume & Leinweber, 2004). Sods of heath and/or forest litter were applied in the stables as fresh animal bedding and at times were spread out on the arable fields, serving as manure (FAO, 2001). Based on soil profile information from the Aardewerk database (Van Orshoven et al., 1988), average plaggen soil thickness in the study area was estimated at 0.40 m. The post-medieval DEM was stripped of this predefined amount in the areas with recorded plaggen soils on the soil map. Due to the nature of the evidence, the exact depth and the location of the plaggen extraction zones are generally not provided in the literature. It is assumed that some 10 ha of heath land were needed to maintain the nutrient level of 1 ha of arable land (FAO, 2001). Based on these arguments (unknown location of the removal sites and relatively low volume to surface ratio in the extraction areas), a positive correction (i.e., adding heights) for the extraction areas was not applied in the reconstruction of the (pre)historic DEM.

**Table III** Reconstructed model input and their corresponding time periods in the modeling.

| Start year | End year | Topography | Vegetation | Recharge | Hydrology | Ditches | $C_{DRAIN}$ |
|---|---|---|---|---|---|---|---|
| 10,766 B.C.E. | 1113 C.E. | (Pre)historic DEM | Varying in time (Figure 1), spatially uniform | 30-year averaged time series, spatially uniform | (Pre)historic network, model parameters from 1924 to 1953 C.E. calibration period | - | Spatially uniform, value calibrated on archaeological and recorded podzol evidence |
| 1114 C.E. | 1803 C.E. | Post-medieval DEM | Deciduous forest, grassland and shrubs | 30-year averaged time series, spatially nonuniform | Present network (FHA), model parameters from 1924 to 1953 C.E. calibration period | Spatially uniform, model parameters from 1924 to 1953 C.E. calibration period | Spatially uniform, value from 1924 to 1953 C.E. calibration period |
| 1804 C.E. 1924 C.E. | 1923 C.E. 1953 C.E. | Present DEM | | | | | |

For areas affected by marine influence originating from storm surges and accompanying flood events from the 13th century onward (northern part of the area; Baeteman, 2006) or late medieval Scheldt influence (northeastern part of the area; Crombé, 2005; Soens, in press), the depth to the pre-alluvial material was derived from the memoir accompanying the soil map and their location was derived from the Quaternary geological map. The post-medieval DEM was stripped of this amount at the defined locations. Because the Holocene, in relative terms, is considered to be a geomorphologically stable period, this (pre)historic DEM was applied in the simulations to the time previous to 1114 A.D. All DEMs were used at the same resolution of the groundwater model (100 m × 100 m).

### *Hydrological network*

Watercourses in the model were classified in five size classes, according to the size of their drainage area and following the legislative classification of watercourses as recorded in the FHA. River model parameters, such as water level, elevation of the riverbed, and hydraulic conductance of the riverbed material, were given a fixed value per class. Only for the class with navigable watercourses were variable values used: the width was measured from colored orthophotographs at several points along the course; water level (a fixed mark controlled by sluices) and water depth (taken as 0.5 m below the maximum allowed ship draught) were derived from the statutory demands (Navigational Map of Belgium, 2006). Drainage of excessive water is now mostly performed by subsurface field drains, but for the pre-1950 period these were absent. A network of artificial ditches served a twofold function: drainage of excess water on the one hand, and to encourage the passage of water toward the groundwater on the other hand. Ditches were taken into account from 1114 C.E. onwards (Table III). Depth (0.9 m below surface) and water level (0.05 m) in the ditches in the model was chosen based on a pilot study (Flemish Government Report, 2001).

The location of the present-day watercourses was taken from the FHA. However, since medieval times, existing watercourses have been modified and new canals constructed, resulting in a present-day river network strongly deviating from the natural system present during prehistoric times. Therefore, a reconstruction of this natural system was conducted based on a twofold analysis: a cartographical analysis and a streamflow calculation, both executed in a GIS. The workflow is presented in Figure 3. In the cartographical analysis the present-day hydrological network as recorded in the FHA, was classified into straight/unnatural and curving/natural looking waterways in a GIS based on a visual screening. Georeferencing of the historical maps was executed whenever possible, although in most cases this was not feasible and a rough estimate of the position of the watercourses was performed based on the available place names. A total of 61 separate waterways located inside the study area were vectorized on the historical maps. The extra information provided by the historical maps was especially valuable in the geographical reconstruction of reaches in a GIS, which are now hidden underground (especially in urban areas), or which are disused due to straightening and canalizing (Figure 4). By combining this with vectorized watercourses from the geomorphological map of

 Copyright © 2013 Wiley Periodicals, Inc.

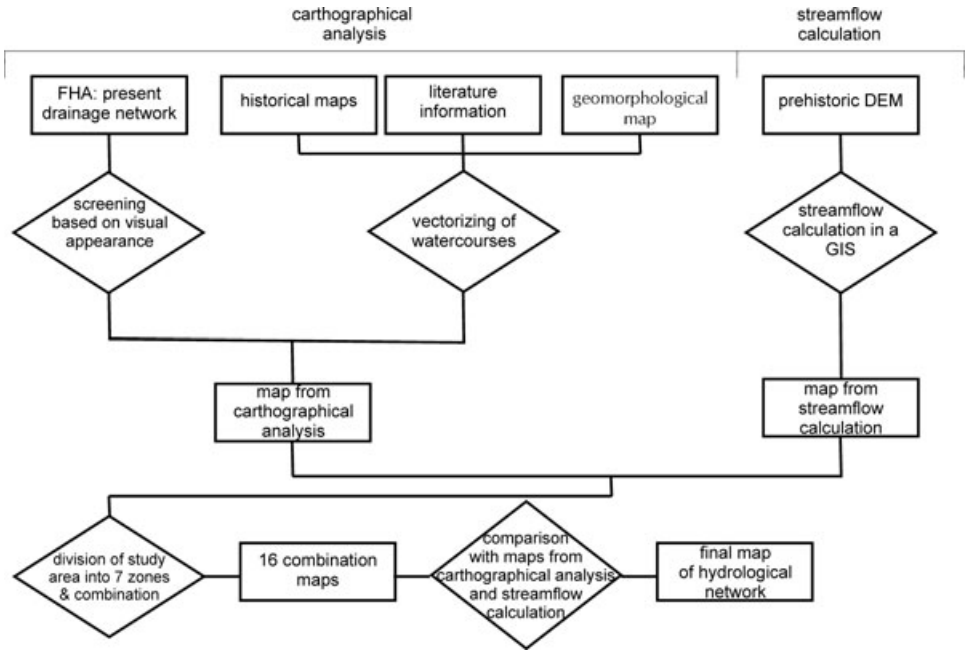


**Figure 3** Flowchart of the hydrological network reconstruction based on cartographical analysis and streamflow calculation.

the study area (De Moor & Heyse, 1994; georeferenced in a GIS), a preliminary map of the hydrological network was constructed (Figure 5A). The streamflow calculation was based on the method presented by Jenson and Domingue (1988), in which stream models are generated starting from topographical data as provided by a DEM (Figure 5B). In this case the (pre)historic DEM was used.

As a result of the visual screening, the map derived from the cartographical analysis (Figure 5A) shows a large area containing no watercourses. Furthermore, the map produced from the streamflow calculation (Figure 5B) reveals straight, unnatural watercourses due to flat surfaces in the DEM restricting the streamflow algorithm. Therefore, new maps of the drainage network were created as unique combinations of the constructed networks of the cartographical analysis and streamflow calculation. To limit the number of combinations, the study area was divided in seven zones based on the geomorphology and hydrology of the region (Figure 5C). Hence, instead of combining each watercourse from both analyses separately, only the watercourses per zone were combined. The combination with the highest sum of overlapping cells with the maps (upscaled to 100 m × 100 m) from the cartographical analyses and streamflow calculation was assumed to represent the (pre)historic drainage network (Table III). River model parameters for the (pre)historic network were indirectly allocated through the five predefined size classes: rivers acquired from the cartographical analysis inherited their present-day classification, but watercourses derived from the streamflow calculation were manually classified.

### *Recharge as a function of changing climate and vegetation type*

Daily values of the recharge to the groundwater table were calculated with a modified Thornthwaite-Mather function, taking the daily precipitation ($P$), potential evapotranspiration ($ET_0$), runoff ($RO$), canopy interception ($I$), and change in soil-water content ($dSW$) into account (Equation 1; Thornthwaite & Mather, 1955, 1957; Steenhuis & Van Der Molen, 1986).

$$\text{Recharge} = P - ET_0 - RO - I - dSW. \quad (1)$$

The daily values were then averaged over 30-year intervals and input into the model. The daily precipitation and daily evapotranspiration series were obtained following the methodology described in Finke and Hutson (2008). Annual precipitation and temperature anomalies for central western Europe and covering the entire study period in 100-year intervals, generated from quantitative palynological analysis following the methodology of Davis et al. (2003) were provided by Davis (personal communication, 2008). By adding current annual values from Merendree-Schipdonk and Uccle to the

 Copyright © 2013 Wiley Periodicals, Inc. 

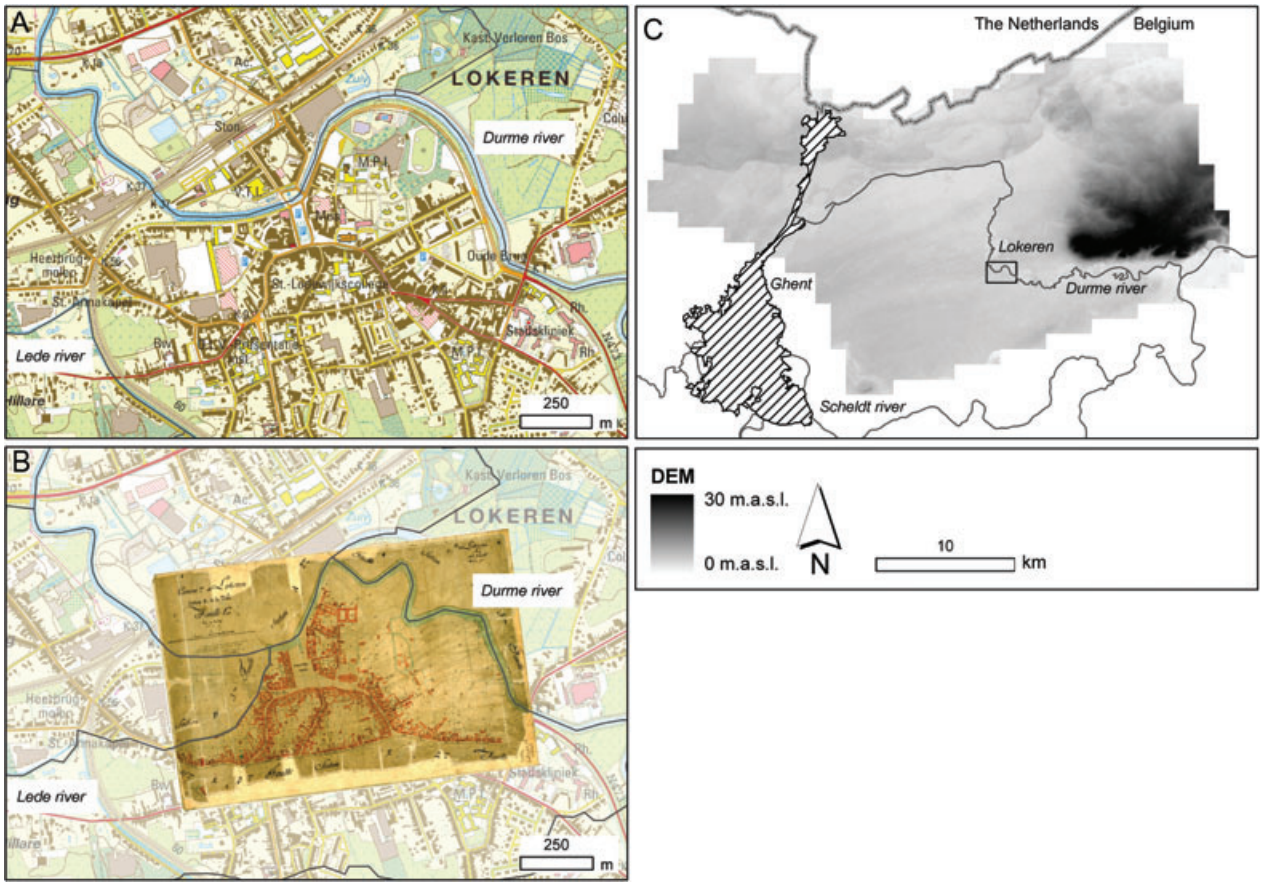


**Figure 4** Man-made modifications of the river Durme at the city of Lokeren. (A) The topographical map of Lokeren (scale 1:10,000) with indication of the present-day rivers Durme and Lede; (B) land register map dating from 1881 C.E., with indication of the former course of the rivers Durme and Lede; (C) localization of the Durme river and the city of Lokeren in the study area.

precipitation and temperature anomalies, local series were obtained. The 100-year intervals were then linearly interpolated to produce continuous series of yearly values. The daily series were calculated by rescaling a standard record of daily values from the weather station so that annual sums of daily values matched the yearly values. This daily temperature series was then used in the equation of Hargreaves and Samani (1985) to calculate daily potential evapotranspiration for 51°N. Yearly values of potential evapotranspiration measured at the weather station of Melle were used to rescale daily potential evapotranspiration values to match the yearly sum.

The temporal sequence of vegetation types in the study area was based on the work of Verbruggen, Denys, and Kiden (1996), who defined the regional vegetation development for northern and middle Belgium, encompassing the study area. For modeling purposes, these defined vegetation types were conceptualized in three vegetation classes: grassland and shrubs, deciduous forest, and coniferous forest (Figure 2; Table III). Geographically, the vegetation was assumed to be uniformly present over the entire study area. Only for more recent times was a heterogeneous distribution of the vegetated surface imposed (Figure 6; Table III): forest versus grassland and shrubs. This was based on the forest distribution maps of De Keersmaeker et al. (2001). In general, runoff and canopy interception, needed in the recharge calculation, are described as fractions of the precipitation and are related to the vegetation type. The runoff on vegetated surfaces was assumed to be negligible (Batelaan, 2006) and applied likewise in the modeling. The canopy interception was set at 0%, 8%, and 12% of the precipitation, for grassland and shrubs, deciduous forest, and coniferous forest respectively, based on the work of Bouten (1992) and Finke (2012a).

 Copyright © 2013 Wiley Periodicals, Inc.

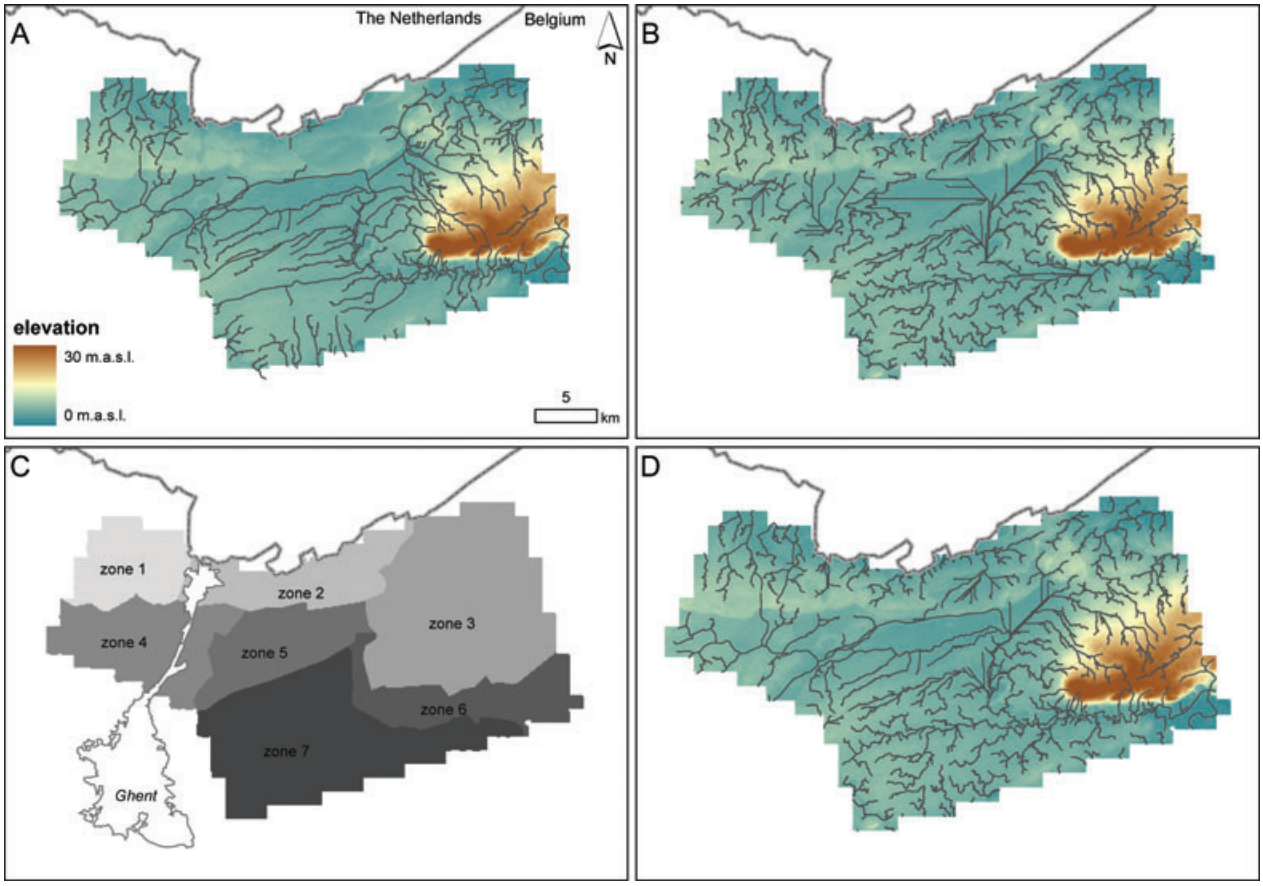


**Figure 5** (A, B) Maps of the hydrological network based on the cartographical analysis and streamflow calculations, respectively; (C) division of the study area into seven zones; (D) the final map of the hydrological network.

## Model Calibration

Information on prehistoric phreatic groundwater levels is practically nonexistent in the literature, and whenever present, it is in most cases of an indirect and dispersed nature, such as the presence of groundwater-fed peat marshes or wells found at archaeological sites. However, intensive peat extraction from the 12th century onwards resulted in large uncertainties in the location, the extent, and the nature and age of the former peat marshes (Jongepier et al., 2011). Furthermore, wells only mark the presence of the water table within a certain range between the surface and the bottom of the well. The model

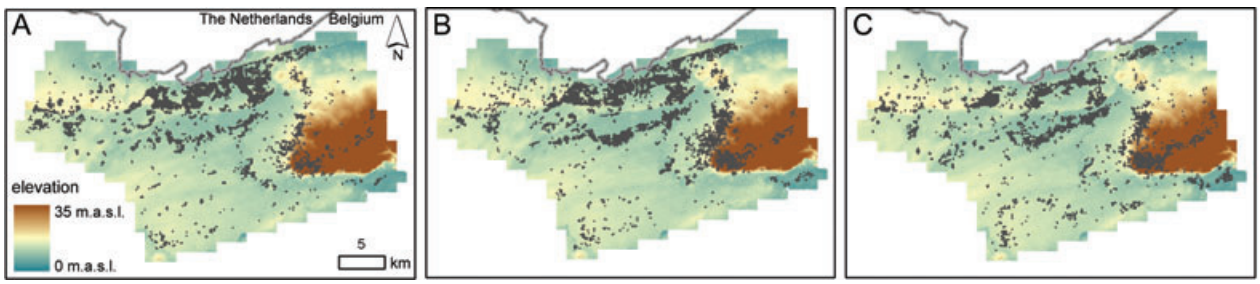


**Figure 6** Distribution of the forested areas (in gray) in the study area for three different periods based on the research of De Keersmaeker et al. (2001). (A) 1114–1803 C.E.; (B) 1804–1923 C.E.; (C) 1924–1983 C.E.

 Copyright © 2013 Wiley Periodicals, Inc. 

**Table IV** Texture and drainage classes with their MHWT and MLWT depth ranges after Ameryckx, Verheye, & Vermeire (1995), as well as their computed mean MHWT depth, mean MLWT depth, MWT depth, and standard deviation ($\sigma$) on the calculated MWT depth. All depths in centimeter below surface.

| | | | | | | | $\sigma_{MWT}$ | |
|---|---|---|---|---|---|---|---|---|
| Text. class | Drain. class | MHWT depth range | Mean MHWT depth | MLWT depth range | Mean MLWT depth | MWT depth | (cm) | (% MWT depth) |
| ZSP | a | >125 | 194.4 | >125 | 246.6 | 220.5 | 100.2 | 45.4 |
| | b | 90–120 | 105.0 | >125 | 182.2 | 143.6 | 43.6 | 30.4 |
| | c | 60–90 | 75.0 | >125 | 157.1 | 116.0 | 27.3 | 23.5 |
| | d | 40–60 | 50.0 | >125 | 140.5 | 95.3 | 15.6 | 16.3 |
| | e | 0–120 | 60.0 | 100–120 | 110.0 | 85.0 | 41.5 | 48.8 |
| | f | 0–100 | 50.0 | 50–100 | 75.0 | 62.5 | 38.1 | 61.0 |
| | g | 0–50 | 25.0 | 0–50 | 25.0 | 25.0 | 24.1 | 96.4 |
| | h | 20–40 | 30.0 | >125 | 128.7 | 79.3 | 9.0 | 11.4 |
| | i | 0–20 | 10.0 | >125 | 121.9 | 66.0 | 6.9 | 10.5 |
| ALEU | a | >125 | NP | >125 | NP | NP | NP | NP |
| | b | >125 | NP | >125 | NP | NP | NP | NP |
| | c | 80–>125 | 92.5 | >125 | 168.3 | 130.4 | 34.0 | 26.1 |
| | d | 50–80 | 65.0 | >125 | 139.2 | 102.1 | 16.6 | 16.3 |
| | e | 0–120 | 60.0 | 80–120 | 100.0 | 80.0 | 43.1 | 53.9 |
| | f | 0–80 | 40.0 | 40–80 | 60.0 | 50.0 | 30.5 | 61.0 |
| | g | 0–40 | 20.0 | 0–40 | 20.0 | 20.0 | 19.3 | 96.4 |
| | h | 20–50 | 35.0 | >125 | 125.4 | 80.2 | 10.9 | 13.6 |
| | i | 0–20 | NP | >125 | NP | NP | NP | NP |

ZSP: texture class of sand (Z), loamy sand (S), and light sandy loam (P); ALEU: texture classes of silt (A), silt loam (L), clay (E), and heavy clay (U); a: excessively drained; b: good drainage; c: moderate drainage; d: insufficient drainage; e: moderately poor drainage; f: poor drainage; g: very poor drainage; h: moderately poor drainage and perched water tables; i: very poor drainage and shallow perched water tables.
NP: not present in the study area.

was therefore calibrated in a two-step approach. First, the 1924–1953 period was calibrated based on comparison with calculated MWT depths and second, a control and extra calibration on the entire period was performed by comparison with archaeological and recorded podzol evidence.

For the 1924–1953 control period, observations on the MWT depth were derived from the soil map drainage classes. At the time of mapping, subsurface field drains were absent so this mapped state is the best recorded representation of the natural state. Each drainage class is related to a mean highest and mean lowest water table (MHWT and MLWT, respectively), expressed as a range of depths below the surface (Ameryckx, Verheye, & Vermeire, 1995; Van Ranst & Sys, 2000; Table IV). For each drainage class, a mean value for the MHWT and MLWT depth was calculated, and the average of both served as the value for the MWT depth. As the augering depth during the soil survey was limited to 1.25 m below surface (Van Ranst & Sys, 2000), the lower boundary of certain classes was not recorded. The missing information was completed with data from a more recent soil drainage class remapping project in the study area (Zidan, 2008). The uncertainty on the calculated MWT depths was calculated based on the assumptions that the MHWT and MLWT depths were normally distributed with a cumulative probability of 70% between the upper and lower bounds. The value of 70% was derived from Dent and Young (1981) concerning the mapping quality of soil surveyors. Using the Z-score, the variance on both MHWT and MLWT depths was computed. The standard deviation on the MWT depth was taken as the square root of the average of both variances (Table IV). The resulting full-coverage data set of MWT depths was randomly split into a calibration and a validation set in a 70/30 ratio (Figure 7). However, in 19.4% of the area, the MWT depth could not be reconstructed. This is due to the presence of urban areas at the time of soil mapping, but also because of the highly industrialized region around the Canal of Ghent-Terneuzen. Furthermore, at the southern border of the Cuesta of Waas (Figure 1B), the MWT depths based on data from the pilot area with a recent drainage class mapping (Zidan, 2008), deviated largely from MWT depth values as calculated in time-series analyses on present-day local measurements (Finke, Van de Wauw, & Baert, 2010).

The calibration of the 1924–1953 time period was conducted on the following model parameters: the hydraulic conductance of the riverbed; the hydraulic conductance of the upper 0.20 m of the soil surface; the transmissivity; and the vertical hydraulic conductivity divided by the thickness of the layers. Only the five upper computational

 Copyright © 2013 Wiley Periodicals, Inc.

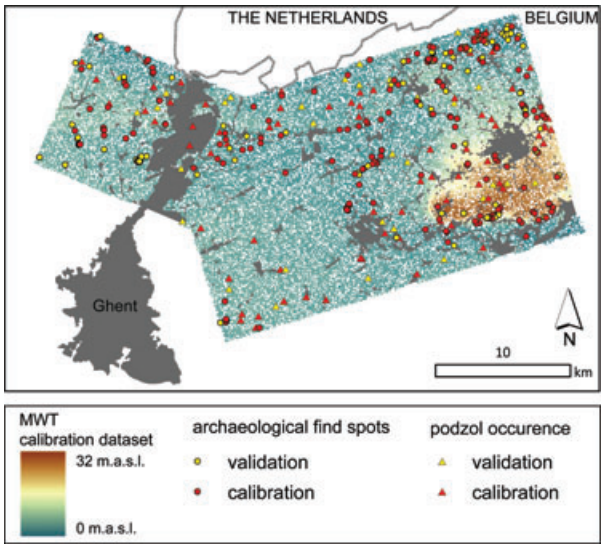


**Figure 7** Calibration (in color scale) and validation (in white) data set of the MWT observations (m.a.s.l.), calculated based on the drainage class map. Calibration and validation data set of the recorded archaeological sites and podzols.

layers (up to 25 m deep) were taken into account during the calibration, since the influence of deeper layers on the phreatic groundwater table appeared to be negligible. This was executed in a manual iterative approach in which the calibration parameters were adjusted and evaluated by comparing the MWT depths based on the drainage class map ($MWT_{i,m}$) with the simulated MWT depths ($MWT_{i,c}$) at locations $i$, based on quantitative error measures (Equations 2–4): root mean square error (RMSE), mean error (ME), and mean absolute error (MAE).

$$\mathrm{RMSE} = \sqrt{1/n \sum_{i=1}^{n} (MWT_{i,m} - MWT_{i,c})^2}, \quad (2)$$

$$\mathrm{ME} = 1/n \sum_{i=1}^{n} (MWT_{i,m} - MWT_{i,c}), \quad (3)$$

$$\mathrm{MAE} = 1/n \sum_{i=1}^{n} \left| MWT_{i,m} - MWT_{i,c} \right|. \quad (4)$$

The final parameter values for the 1924–1953 calibration period were then used in the simulations for the entire study period. However, through time, land use and land management have changed (e.g., the loss of forested area due to the expansion of built-on and cultivated land, or the presence of ditch networks that did not exist in prehistoric times). Therefore, it was concluded that a further calibration of hydraulic conductance of the upper 0.20 m of the soil surface ($C_{\mathrm{DRAIN}}$) was necessary in relation to the presence of archaeological findings (Gyucha et al., 2011). In this research we used Mesolithic and Neolithic find spots, Bronze Age barrows, Late Iron Age and Roman Age sites, and recorded podzol locations. All sites belonging to one archaeological period were split randomly into a calibration (70%) and validation (30%) data set, to ensure that each of these archaeological periods was represented. Afterwards, final calibration and validation data sets (Figure 7) were produced by combining the separate sets. Assuming that the difference between MHWT and MWT, as recorded at the time of soil mapping, was the same in prehistoric times, the MHWT at the archaeological sites was calculated from the simulated MWT. The number of archaeological sites at which a calculated MHWT was below the surface served as a criterion in this prehistoric calibration. The adjustment of $C_{\mathrm{DRAIN}}$ was performed with a fixed amount in a manual iterative procedure and stopped when the change in number of sites meeting the criterion was below 0.3%.

The presence of podzols served as a second control on the prehistoric simulated water tables. Point locations with well-developed podzols (marked Bh and Bhs horizons) were collected from the Aardewerk database. This data set was randomly split into a calibration and validation part, containing 70% and 30%, respectively, of the recorded podzol profiles (Figure 7). These locations were then evaluated according to the following criterion: MLWT must be lower than the bottom of these B-horizons for at least 1500 years (Jacques et al., 2010). This was based on the reasoning that clearly recognizable podzol-Bh(s) horizons have formed in profile parts that are above the water table at least part of the year. Based on the assumption that prehistoric MLWT deviated equally from the MWT, as during the time of soil mapping, this difference was calculated and subtracted from the simulated MWT to obtain a value for the MLWT. The calibration was performed by only adjusting the parameter $C_{\mathrm{DRAIN}}$ by a fixed amount, in a manual iterative approach. The final value for $C_{\mathrm{DRAIN}}$ was then chosen when no change in the number of sites with recorded podzols occurred for several iterations.

## RESULTS AND DISCUSSION

### Uncertainties in the Reconstructed Boundary Conditions and Model Limitations

Input errors affect the initial state of the model and the model boundary conditions along the time period covered with the simulations. Ideally, this uncertainty is estimated via uncertainty analysis; however, when time variant boundary conditions and associated uncertainties are present, this becomes extremely complex (Finke, 2012b)

 Copyright © 2013 Wiley Periodicals, Inc. 

and is therefore not applied in this research. An initial estimation of the model quality is therefore provided by listing the uncertainties of the various (reconstructed) model inputs (Table I).

The LiDAR data have a planimetric accuracy in the order of 0.50 m and an altimetric accuracy ranging from 0.07 m on a concreted surface to 0.20 m on vegetation cover (Werbrouck et al., 2011) at point scale. The accuracy of the present DEM is better than the one from the LiDAR data as errors level each other out during the upscaling. This planimetric accuracy is also applicable to the post-medieval and (pre)historic DEM. Of course, due to the filtering of anthropogenic artifacts and subsequent interpolation during the creation of the post-medieval DEM, small errors in the elevation values could have been induced. We assume these to be lower than 0.20 m. Embankments around rivers remain regions of higher uncertainty. Today, due to channels silting up, the river Durme has a higher elevation than its surroundings. Areas where vectorized contours of historical maps were used in the interpolation have a minimum accuracy of 1 m, which is the maximum equidistance between the contours. Furthermore, agricultural and construction activities in the study area have leveled the terrain and largely removed previous microtopography. However, the use of 100 m $\times$ 100 m grid cells largely averages out these local height differences and averaged errors are small. Plaggen depths and depths to pre-alluvial sediments were derived from the Aardewerk database and other information collected during the national soil survey campaign. We believe the recorded depths are accurate at 0.10 m. Furthermore, it was noted that the location of plaggen extraction sites is often unknown, while the extraction areas were generally much larger than the application areas (FAO, 2001). Therefore, this uncertainty is estimated at 0.05 m. Streamflow calculations on a DEM in a GIS are commonly executed in the reconstruction of hydrological networks (e.g., Colombo et al., 2007; Mandlburger et al., 2011). However, knowledge on hydrological palaeocharacteristics is scarce and very little research has been carried out on the effect of climate change on the relationship between surface waters and aquifers that are hydraulically connected (Alley, 2001).

It was concluded by Davis et al. (2003) that the effect of nonclimatic and local climatic factors on their methodology to reconstruct temperature anomaly series was limited. Their evaluation was based on internal consistency and agreement with other proxy records provided in the literature. In relation to the precipitation anomalies, this conclusion is assumed to be applicable as well since the reconstruction was performed following the same method. The anomalies were adjusted to local conditions based on present-day meteorological measurements with high accuracy. Ideally, series calculated from proxies on more local samples could lead to a refinement of the recharge data. Unfortunately, such climatic series are not yet available for the study area. The errors of the reconstructed yearly precipitation and evapotranspiration were both estimated to be less than 50 mm and the errors of the reconstructed January and July temperatures are less than 2°C (Zwertvaegher et al., 2010). Canopy interception values found in the literature cover a broad range depending on, for example, forest density, tree species, season, rainfall intensity, and wind speed (Hörmann et al., 1996; Price & Carlyle-Moses, 2003; Herbst et al., 2008). This of course also influences the recharge reconstruction. As a check, calculated recharge for the 1954–1983 period (216.8 mm $yr^{-1}$) was compared to the present average value for Flanders (222 mm $yr^{-1}$; VMM, 2006). It was concluded that both values are of comparable order.

The available reconstructions limit the length of the study period. The Late Glacial is known as a highly dynamic period for which intense aeolian phases with coversand deposition and erosion (Kasse et al., 2007; Derese et al., 2010; Crombé et al., 2012) and large modifications in the river systems are recorded (De Smedt et al., 2012). Therefore, we started the study period at the very end of the Late Glacial and with a major focus on the Holocene. Relative to the profound changes of the Late Pleistocene, the Holocene may be regarded as a much more geomorphologically stable period.

## Model Quality

It is important to point out that the model, even after calibration, is not free from error. This starts with the measured observations against which the model is calibrated. For example, for the drainage classes representing moderately poor to very poor drainage conditions, the standard deviation on the MWT depths, derived from the drainage classes in the soil map, is near to or more than 50% (Table IV). However, these only cover a small part of the study area.

Model quality for the 1924–1953 time period is expressed as quantitative error measures as ME, MAE, and RMSE (Table V). The calibration and validation results show good agreement. The ME is close to zero, in the order of several centimeters. The RMSE is in the range of several tens of centimeter. Figure 8 shows the MWT values based on the drainage class map and the simulated values of the MWT for the 1924–1953 period at the calibration locations ($R^2 = 0.9765$). The deviation between simulated values and values obtained from the drainage class map increases as both values increase. This can be related to erroneous simulated MWT values in the region of the Cuesta of Waas (indicated as subarea 3,

 Copyright © 2013 Wiley Periodicals, Inc.

**Table V** Model performance for the 1924–1953 calibration period: mean of the simulated MWT depth (mean) and standard deviation ($\sigma$). ME, MAE, and RMSE based on the simulated MWT depths and the MWT depths at the calibration and validation locations (calculated based on the drainage class map). No. of locations (%) of the calibration and validation data sets of archeological sites and well-drained podzols meeting the criteria after the prehistoric calibration of $C_{DRAIN}$. Location of subareas 1–3 is indicated in Figure 1B.

| | | | | Entire area | Subarea 1 | Subarea 2 | Subarea 3 |
|---|---|---|---|---|---|---|---|
| *MWT depth* | *All data* | *Mean* | *m* | 1.119 | 1.098 | 0.904 | 1.377 |
| | | $\sigma$ | *m* | 0.957 | 0.575 | 0.435 | 1.407 |
| | *Cal.* | *ME* | *m* | 0.012 | −0.013 | 0.110 | −0.077 |
| | | *MAE* | *m* | 0.439 | 0.354 | 0.301 | 0.661 |
| | | *RMSE* | *m* | 0.660 | 0.484 | 0.398 | 0.939 |
| | *Val.* | *ME* | *m* | 0.018 | −0.006 | 0.117 | −0.070 |
| | | *MAE* | *m* | 0.437 | 0.350 | 0.302 | 0.656 |
| | | *RMSE* | *m* | 0.656 | 0.488 | 0.397 | 0.931 |
| *Archaeological sites* | *Cal.* | *No. of sites meeting a fixed criterion* | *%* | 92.42 | - | - | - |
| | *Val.* | | *%* | 96.28 | - | - | - |
| *Recorded podzol locations* | *Cal.* | | *%* | 90.79 | - | - | - |
| | *Val.* | | *%* | 96.88 | - | - | - |

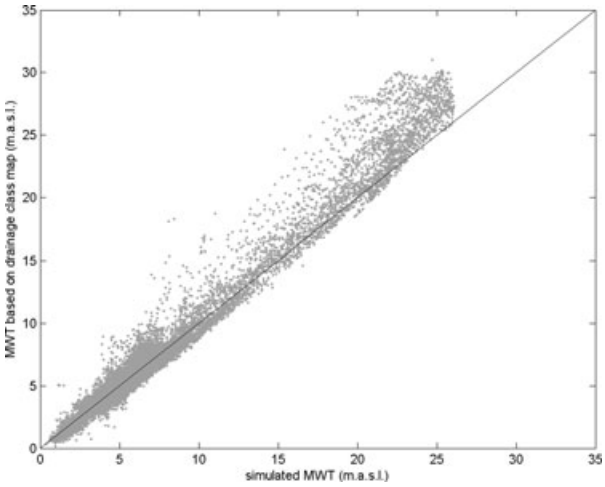


**Figure 8** MWT values calculated based on the drainage class map (m.a.s.l.) versus simulated MWT values at the locations of the calibration data set (gray dots). Black line: line of perfect agreement.

Figure 1B), or due to erroneous values in the calculated MWT observation data set based on the mapped drainage classes in the same region. The latter could relate to the fact that data from the recent drainage class mapping in the pilot area, used to complete the missing information in the construction of the MWT observation data set, would not be applicable to this cuesta area (subarea 3). Furthermore, the calibration of the prehistoric MWTs was based on adjusting the $C_{DRAIN}$ function of the percentage of archaeological sites and recorded podzol locations meeting a fixed criterion. The number of calibration sites meeting the criterion at the final $C_{DRAIN}$ is above 96% (Table V). The number of accepted validation sites is even slightly larger than for the calibration sites, this is true for both the archaeological sites as for the locations with recorded podzols. It is possible that nonaccepted sites probably lie within a heterogeneous area (archaeological/recorded podzol site on higher ground surrounded by lower ground). Such detail can be lost due to the resolution (100 m × 100 m) of the modeling. Downscaling the maps of the MWT depths to a higher resolution may yield even better results. This is yet to be tested.

## Spatial and Temporal Variations in MWT Depth

The output of the phreatic palaeogroundwater modeling consists of a series of full-coverage maps of the MWT depth spanning the entire study period. The temporal evolution of the MWT depth (Figure 9A) reflects generally the calculated recharge (Figure 9B), and hence the climate. At the start of the Younger Dryas, the level of the MWT falls to reach its minimum around the middle of the Younger Dryas, generally climbing to higher phreatic groundwater levels throughout the Preboreal and Boreal. The transition between the Boreal and Atlantic is characterized by an increase in the MWT depth, but from the Atlantic onwards, the MWT remains at a fairly constant level. The influence of the present-day drainage system and land use is reflected by an increase in MWT depth from 1114 A.D. onwards. Likely within-year fluctuations, indicated by MHWT and MLWT depths (Figure 9A), are calculated from the simulated MWT depths. This calculation was based on the assumption that their deviation from the MWT depth in previous times equals the difference with the MWT depth, as recorded at the time of soil mapping.

The full-coverage maps of the MWT depth show a dry situation in practically the whole area in the Younger

 Copyright © 2013 Wiley Periodicals, Inc. 

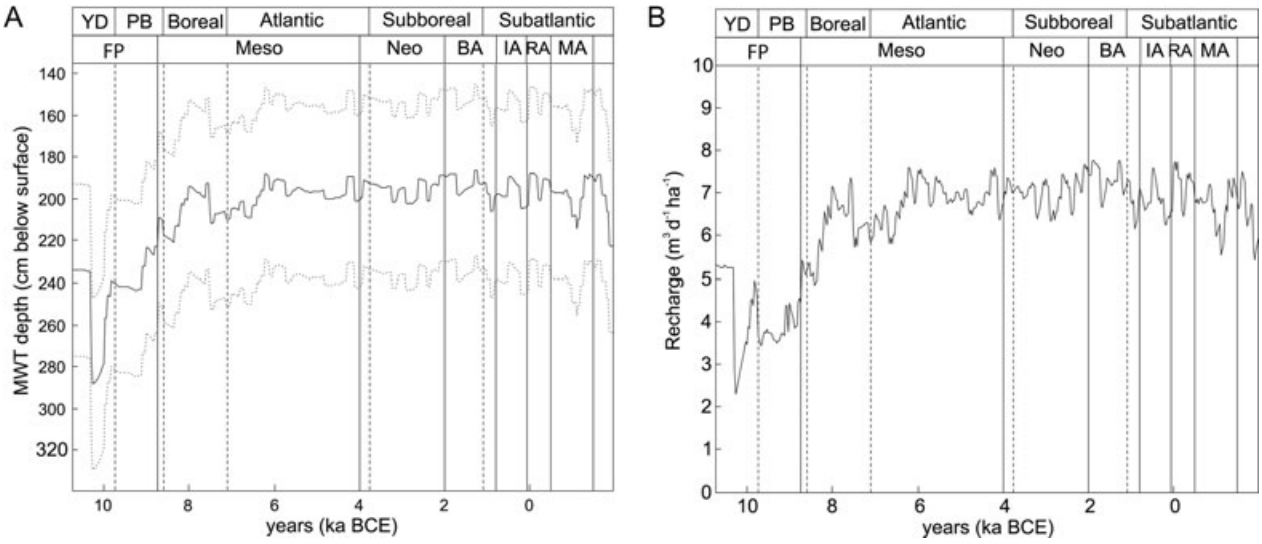


**Figure 9** (A) Time series of the simulated MWT depth (solid line) for a location on the coversand area. Calculated MHWT and MLWT depths are also indicated as upper and lower dashed lines. (B) Time series of the calculated recharge ($m^3$ $d^{-1}$ $ha^{-1}$). Chronostratigraphical (dashed vertical lines) and archaeological periods (as defined for Sandy Flanders; solid vertical lines) are indicated on top of each graph: YD, Younger Dryas; PB, Preboreal; FP, Final Palaeolithic; Meso, Mesolithic; Neo, Neolithic; BA, Bronze Age; IA, Iron Age; RA, Roman Ages; MA, Middle Ages.

Dryas (Figure 10). The average MWT depth in the region is deeper than 1.20 m. However at the southern border of the coversand ridge, a slightly wetter area remains (average MWT depth between 0.20 and 0.60 m). From the Younger Dryas, throughout the Preboreal to the Boreal, a fall in the phreatic water table depth occurs. The coversand ridge persists as a dry region in the landscape, bordered to its south by a small area with shallow groundwater tables. In the south an area occurs where, especially from the Boreal onwards, both shallow and deep groundwater tables occur within a very short distance. This region is characterized by small parallel ridges and depressions as the remainders of a braided river system. For the rest of the Holocene, the MWT depth is rather constant, as is the climate influencing the recharge. However, if deforestation and reforestation history between Bronze and Middle Ages were known, this would probably have resulted in (nonforested) areas with higher water tables due to lower interception. Because of the implementation of drainage ditches, the 1950 situation (Figure 10D) is slightly drier compared to the prehistoric periods, especially in the lower-lying areas.

## MWT in a Geoarchaeological Context

In the study area, the archaeological sites dating to the Early Mesolithic (Figure 10B) are mostly located on the southern border of the coversand ridge of Maldegem-Stekene. This is an interesting location due to the gradient in MWT depths when crossing the ridge in a southerly direction. The archaeological sites are positioned on the drier ridge, with possible freshwater seepage in the vicinity at the southern border. Also, a number of sites are located on the drier grounds bordering the river Kale/Durme. The transition from the Boreal to the Atlantic is characterized by a slight drying and coincides with a marked decrease in sites dating to the Middle Mesolithic (Figure 10C; Crombé et al., 2011). This could indicate that the water level in the area, especially in the river channel, limited the availability of drinking water. For the Atlantic period, again slightly higher groundwater levels are found as compared to the Boreal-Atlantic transition. Simultaneously the number of sites dating to the Late Mesolithic increases even though the density is no longer comparable to the Early Mesolithic. Although sites remain associated with drier positions in the vicinity of wetter locations, such as the southern border of the coversand ridge and the Kale/Durme riverbanks, Late Mesolithic sites tend to be found at important nodal positions, a pattern which persists during the Neolithic. According to Crombé et al. (2011) this might be linked to an increased emphasis on wetland exploitation, including fishing, which resulted in a reduction in group mobility. From the Atlantic onwards the simulated MWT depths remain quite constant. The Bronze Age barrows on the other hand, do cover this dune complex area as well as further away from its southern border, while Late Iron

 Copyright © 2013 Wiley Periodicals, Inc.

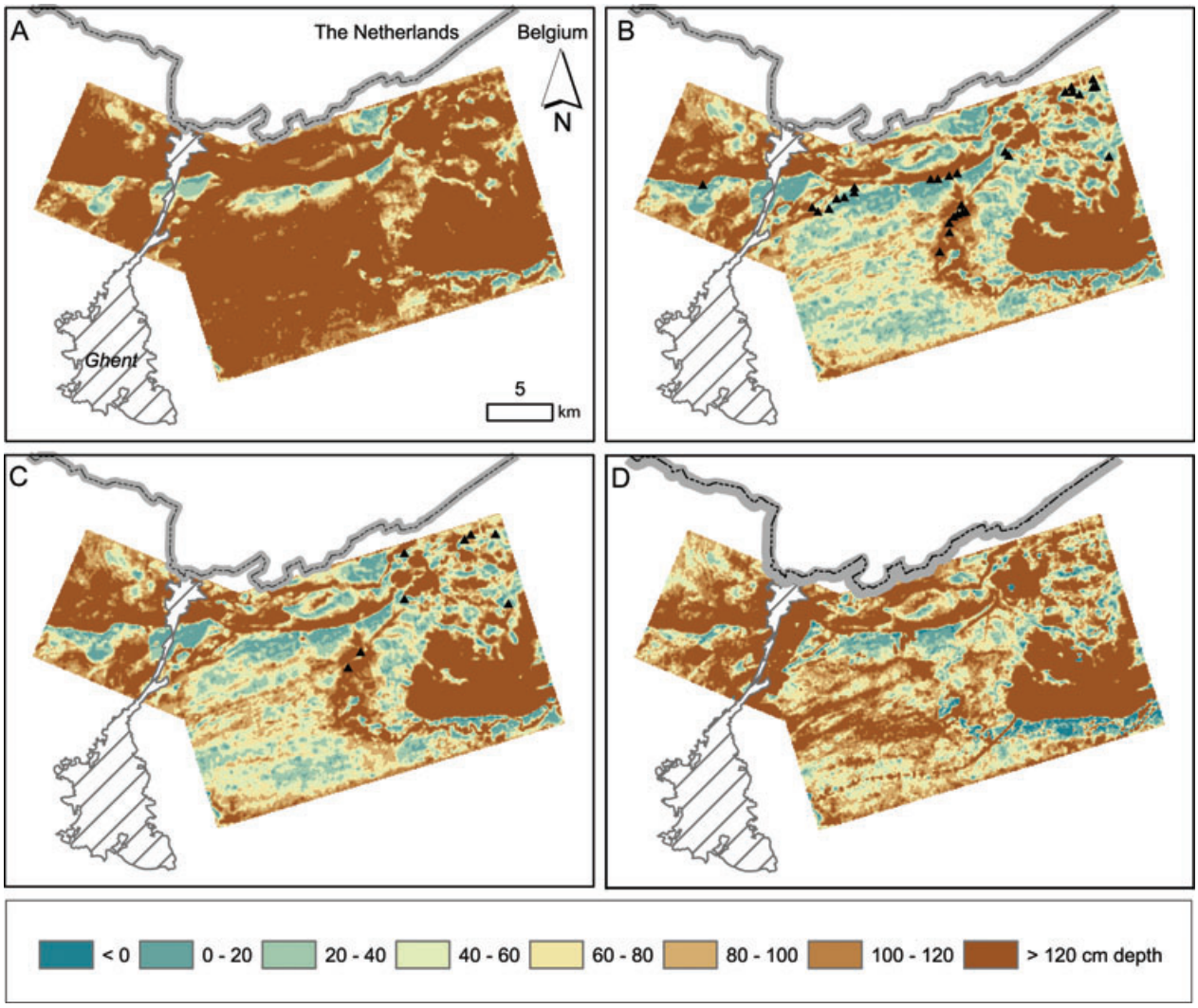


**Figure 10** Full-coverage maps of the MWT depth (expressed in cm below the surface). (A) 10.15 ka B.C.E. (Younger Dryas); (B) 7.84 ka B.C.E. (Boreal), with Early Mesolithic find spots (black triangles); (C) 7.12 ka BCE (Boreal-Atlantic transition), with Middle Mesolithic find spots (black triangles); (D) time of soil mapping (1950 C.E.).

Age and Roman find spots are not found here. The Roman sites are mainly located in the cuesta region.

However, one region in particular remains devoid of archaeological evidence throughout all periods investigated: it concerns the area of parallel ridges and depressions, to the south of the Moervaart depression. The question arises as to how far this is a reflection of the archaeological reality or of a biased impression due to poor preservation of the archaeological remains under the influence of natural degradation, along with the urbanization and industrialization of the region. This phenomenon was investigated for the Bronze Age barrows, but no clear answer could be given due to rather unsuccessful aerial surveys and only a limited number of sites revealed at recent excavation projects, only bordering the region under question (De Reu et al., in press). Today this area is characterized by a dense network of small brooks and ditches. In the 1960s, the poor condition of this network could lead to seasonally high groundwater tables and even flooding of the neighboring areas in winter (Ameryckx & Leys, 1962). In earlier times when the artificial drainage network was absent, this must have been the case. Parallel higher and drier ridges separate the lower and wetter depressions. However, they are of a rather limited extent and hence probably did not serve as good locations for settlement. In addition, the absence of major open water systems, such as lakes and large streams, might have restricted the occupation of this area.

 Copyright © 2013 Wiley Periodicals, Inc. 

## CONCLUSIONS

Palaeogroundwater modeling was performed for Sandy Flanders resulting in a series of full-coverage maps of the MWT depth spanning a time period of 12,720 years, starting in the Younger Dryas, and covering almost the entire Holocene, up to 1953. Calibration for the modern period (1924–1953) was performed using drainage class information from the soil map of Flanders. The model quality for the validation data set (ME of 1.8 cm and RMSE of 65.6 cm) indicates that the model predicts well the phreatic MWTs at the time of soil mapping. Evidence on the past landscape such as archaeological sites and recorded podzol locations were used to further calibrate and validate the model for prehistoric times by adjusting the hydraulic conductance of the upper 0.20 m of the soil ($C_{DRAIN}$): at 96.28% of the archaeological sites and at 96.88% of the podzol locations of the validation data set, the simulated water table depths were in agreement with settlement and podzolization conditions. Difficulties reconstructing the past topographies, drainage network, vegetation type, and climate, based on the current knowledge, are discussed. Application of the model provided an extensive full-coverage data set on the palaeo-MWT, showing a decrease in MWT depth from Younger Dryas to Boreal, and relatively stable MWT depths for the rest of the Holocene. A first analysis indicates that locations with strong MWT gradients seem to be attractive to Mesolithic and Neolithic humans. For later archaeological periods this situation is not as clear. The maps of the MWT can be further investigated in a geoarchaeological and land evaluation context and can be used in, for example, predictive modeling.

The authors gratefully acknowledge Ghent University Integrated Project BOF08/GOA/009 "Prehistoric settlement and land-use systems in Sandy Flanders (NW Belgium): a diachronic and geoarchaeological approach" for financially supporting this work. Our thanks also go to Ilke Werbrouck and Jason Jongepier for the collection of the historical maps used in this study, to Tim Soens for sending us a first draft of his manuscript, and to B. Davis for supplying the January and July temperature anomaly data for central Western Europe and the precipitation data for the same regions. Furthermore, our gratitude goes to two anonymous reviewers for providing very useful comments on an earlier version of this manuscript.

### REFERENCES

Alley, W.M. (2001). Ground water and climate. Ground Water, 39, 161.

Ameryckx, J., & Leys, R. (1962). Verklarende tekst bij het kaartblad Zeveneken 41 W. Bodemkaart van België. Brussel: Instituut tot aanmoediging van het Wetenschappelijk Onderzoek in Nijverheid en Landbouw.

Ameryckx, J., Verheye, W., & Vermeire, B. (1995). Bodemkunde: bodemvorming, bodemeigenschappen, de bodems van België, bodembehoud en -degradatie, bodembeleid en bodempolitiek. Gent.

Baeteman, C. (2006). De laat holocene evolutie van de Belgische kustvlakte: Sedimentatie-processen versus zeespiegelschommelingen en Duinkerke transgressies. In A.M.J. de Kraker & G.J. Borger (Eds.), Veen-Vis-Zout. Landschappelijke dynamiek in de zuidwestelijke delta van de Lage Landen (pp. 1–18). Amsterdam: Geoarcheologische en Bioarcheologische Studies 8, Vrije Universiteit Amsterdam.

Batelaan, O. (2006). Phreatology. Characterizing groundwater recharge and discharge using remote sensing, GIS, ecology, hydrochemistry and groundwater modelling. Unpublished doctoral dissertation, Vrije Universiteit Brussel, Brussels.

Blume, H.-P., & Leinweber, P. (2004). Plaggen soils: Landscape history, properties, and classification. Journal of Plant Nutrition and Soil Science, 167, 319–327.

Bourgeois, J., & Cherretté, B. (2005). L' âge du Bronze et le premier âge du Ferdans les Flandres Occidentale et Orientale (Belgique): un état de la question. In J. Bourgeois & M. Talon (Eds.), L' âge du Bronze du nord de la France dans son context européen. Actes des congrèsnation aux des societies historiques et scientifiques, 125$^{e}$ Lille, 2000 (pp. 43–81). Paris: CTHS.

Bourgeois, I., Cherretté, B., & Bourgeois, J. (2003). Bronze Age and Iron Age settlements in Belgium. An overview. In J. Bourgeois, I. Bourgeois, & B. Cherretté (Eds.), Bronze Age and Iron Age Communities in North-Western Europe (pp. 175–190). Brussels: KVABWK.

Bouten, W. (1992). Monitoring and modelling forest hydrological processes in support of acidification research. Unpublished doctoral dissertation, Fysisch Geografisch en Bodemkundig Laboratorium, Universiteit van Amsterdam, Amsterdam.

Colombo, R., Vogt, J.V., Soille, P., Paracchini, M.L., & de Jager, A. (2007). Deriving river networks and catchments at the European scale from medium resolution digital elevation data. Catena, 70, 296–305.

Crombé, P. (2005). The last hunter-gatherer-fishermen in Sandy Flanders (NW Belgium). The Verrebroek and Doel excavation Projects. Ghent: Archaeological Reports Ghent University 3, Ghent University.

Crombé, P., & Sergant, J. (2008). Tracing the Neolithic in the lowlands of Belgium: The evidence from Sandy Flanders. In H. Fokkens, B.J. Coles, A.L. Van Gijn, J.P. Kleijne, H.H. Ponjee, & C.G. Slappendel (Eds.), Between foraging and farming. An extended broad spectrum of papers presented to Leendert Louwe Kooijmans (pp. 75–84). Leiden: Leiden University.

Crombé, P., & Verbruggen, C. (2002). The Late Glacial and Early Post Glacial occupation of northern Belgium: The evidence from Sandy Flanders. In B.V. Eriksen & B. Bratlund (Eds.), Recent studies in the Final Palaeolithic of

 Copyright © 2013 Wiley Periodicals, Inc.

the European plain. Proceedings of a U.I.S.P.P. Symposium, Stockholm, 14–17 October 1999 (pp. 165–180). Stockholm: Jutland Archaeological Society.

Crombé, P., Sergant, J., Robinson, E., & De Reu, J. (2011). Hunter-gatherer responses to environmental change during the Pleistocene-Holocene transition in the southern North Sea basin: Final Palaeolithic-Final Mesolithic land use in northwest Belgium. Journal of Anthropological Archaeology, 30, 454–471.

Crombé, P., Van Strydonck, M., Boudin, M., Van den Brande, T., Derese, C., Vandenberghe, D., Van den haute, P., Court-Picon, M., Verniers, J., Bos, J.A.A., Verbruggen, F., Antrop, M., Bats, M., Bourgeois, J., De Reu, J., De Maeyer, P., De Smedt, P., Finke, P.A., Van Meirvenne, M., & Zwertvaegher, A. (2012). Absolute dating ($^{14}$C and OSL) of the formation of coversand ridges occupied by prehistoric hunter-gatherers in NW Belgium. Radiocarbon, 54(1), 715–726.

Davis, B.A.S., Brewer, S., Stevenson, A.C., Guiot, J., & Data Contributors. (2003). The temperature of Europe during the Holocene reconstructed from pollen data. Quaternary Science Reviews, 22, 1701–1716.

De Clercq, W. (2009). Lokale gemeenschappen in het imperium Romanum. Transformaties in de rurale bewoningsstructuur en de materiële cultuur in de landschappen van het noordelijk deel van de civitas Menapiorum (Provincie Gallia-Belgica, ca. 100 v. Chr. – 400 n. Chr. Unpublished doctoral dissertation, Ghent University, Ghent.

De Keersmaeker, L., Rogiers, N., Lauriks, R., & De Vos, B. (2001). Ecosysteemvisie Bos Vlaanderen, Ruimtelijke uitwerking van de natuurlijke bostypes op basis van bodemgroeperingseenheden en historische boskaarten. Eindverslag van project VLINA C97/06, studie uitgevoerd voor rekening van de Vlaamse Gemeenschap binnen het kader van het Vlaams Impulsprogramma Natuurontwikkeling in opdracht van de Vlaamse minister bevoegd voor natuurbehoud. Brussel: Instituut voor Bosbouw en Wildbeheer.

De Moor, G., & Heyse, I. (1974). Lithostratigrafie van de Kwartaire afzettingen in de overgangszone tussen de kustvlakte en de Vlaamse Vallei in Noordwest België. Natuurwetenschappelijk Tijdschrift, 56, 85–109.

De Moor, G., & Heyse, I. (1978). De morfologische evolutie van de Vlaamse vallei. De Aardrijkskunde, 4, 343–375.

De Moor, G., & Heyse, I. (1994). Geomorfologische Kaart, Kaartblad Lokeren. Brussel: Ministerie van de Vlaamse Gemeenschap.

De Moor, G., & van de Velde, D. (1995). Toelichting bij de Quartairgeologische Kaart. Kaartblad 14: Lokeren. Brussel: Universiteit Gent, Ministerie van de Vlaamse Gemeenschap – Afdeling Natuurlijke Rijkdommen en Energie.

De Reu, J., Bats, M., De Smedt, P., Bourgeois, J., Antrop, M., Court-Picon, M., De Maeyer, P., Finke, P.A., Van Meirvenne, M., Verniers, J., Werbrouck, I., Zwertvaegher, A., & Crombé, P. (2010). Bronze and Iron Age landscapes in Sandy Flanders (NW-Belgium): A geoarchaeological approach. Lunula, Archaeologia protohistorica, 18, 17–22.

De Reu, J., Bats, M., Crombé, P., Antrop, M., Court-Picon, M., De Maeyer, P., De Smedt, P., Van Meirvenne, M., Verniers, J., Werbrouck, I., Zwertvaegher, A., & Bourgeois, J. (2011a). Een GIS benadering van de bronstijdgrafheuvel in Zandig-Vlaanderen: enkele voorlopige resultaten (België). Lunula, Archaeologia protohistorica, 19, 3–8.

De Reu, J., Bourgeois, J., Bats, M., De Smedt, P., Gelorini, V., Zwertvaegher, A., Antrop, M., De Maeyer, P., Finke, P.A., Van Meirvenne, M., Verniers, J., & Crombé, P. (in press). Beyond the unknown. Understanding prehistoric patterns in the metropolitan landscape. Journal of Historical Geography.

De Reu, J., Bourgeois, J., De Smedt, P., Zwertvaegher, A., Antrop, M., Bats, M., De Maeyer, P., Finke, P.A., Van Meirvenne, M., Verniers, J., & Crombé, P. (2011b). Measuring the relative topographic position of archaeological sites in the landscape, a case study on the Bronze Age barrow in northwest Belgium. Journal of Archaeological Science, 38, 3435–3446.

De Reu, J., Deweirdt, E., Crombé, P., Bats, M., Antrop, M., Court-Picon, M., De Maeyer, P., De Smedt, P., Finke, P., Van Meirvenne, M., Verniers, J., Werbrouck, I., Zwertvaegher, A., & Bourgeois J. (2011c). Les tombelles de l'âge du bronze en Flandre sablonneuse (nord-ouest de la Belgique) : un status quaestionis. Archäologisches Korrespondenzblatt, 41, 491–505.

De Smedt, P., Van Meirvenne, M., Davies, N.S., Bats, M., Saey, T., De Reu, J., Meerschman, J., Gelorini, V., Zwertvaegher, A., Antrop, M., Bourgeois, J., De Maeyer, P., Finke, P.A., Verniers, J., & Crombé, P. (2012). A multidisciplinary approach for reconstructing Late Glacial and Early Holocene landscapes. Journal of Archaeological Science, 40, 1260–1267.

Dent, D., & Young, A. (1981). Soil survey and land evaluation. London, UK: George Allen and Unwin.

Derese, C., Vandenberghe, D.A.G., Zwertvaegher, A., Verniers, J., Crombé, P., & Van den haute, P. (2010). The timing of aeolian events near archaeological settlements around Heidebos (Moervaart area, N Belgium). Netherlands Journal of Geosciences—Geologie en Mijnbouw, 89, 173–186.

FAO. (2001). Lecture notes on the major soils of the world. World soil resources reports, 94.

Finke, P.A. (2012a). Modeling the genesis of luvisols as a function of topographic position in loess parent material. Quaternary International, 265, 3–17.

Finke, P.A. (2012b). On digital soil assessment with models and the pedometrics agenda. Geoderma, 171–172, 3–15.

Finke, P.A., & Hutson, J.L. (2008). Modelling soil genesis in calcareous loess. Geoderma, 145, 462–479.

Finke, P.A., Brus, D.J., Bierkens, M.F.P., Hoogland, T., Knotters, M., & de Vries, F. (2004). Mapping groundwater

dynamics using multiple sources of exhaustive high resolution data. Geoderma, 123, 23–39.

Finke, P.A., Van de Wauw, J., & Baert, G. (2010). Development and testing of a method to update the drainage class map of Flanders. Final report (in Dutch). Ghent: Ghent University.

Flemish Government Report. (2001). Report WAT/L 2000 S 0002 X, Herwaardering van het grachtenstelsel. Fase 2 – Inventarisatie en opbouw van een GIS. Deel uitvoering. Brussel: Department Environment and Infrastructure, AMINAL—Division Water.

Gyucha, A., Duffy, P.R., & Frolking, T.A. (2011). The Körös Basin from the Neolithic to the Hapsburgs: Linking settlement distributions with pre-regulation hydrology through multiple data set overlay. Geoarchaeology, 26, 392–419.

Harbaugh, A.W., & McDonald, M.G. (1996). User's documentation for the U.S. Geological Survey modular finite-difference ground-water flow model. Open-File Report 96–485. Reston, Virginia: U.S. Geological Survey.

Hargreaves, G.H., & Samani, Z.A. (1985). Reference crop evapotranspiration from temperature. Applied Engineering in Agriculture, 1, 96–99.

Herbst, M., Rosier, P.T.W., McNeil, D.D., Harding, R.J., & Gowing, D.J. (2008). Seasonal variability of interception evaporation from the canopy of a mixed deciduous forest. Agricultural and Forest Meteorology, 148, 1655–1667.

Heyse, I. (1979). Bijdrage tot de geomorfologische kennis van het Noordwesten van Oost-Vlaanderen. Brussel: Paleis der Academiën.

Hoek, W.Z. (2001). Vegetation response to the ~14.7 and ~11.5 ka cal. BP climate transitions: Is vegetation lagging climate? Global and Planetary Change, 30, 103–115.

Hörmann, G., Branding, A., Clement, T., Herbst, M., Hinrichs, A., & Thamm, F. (1996). Calculation and simulation of wind controlled canopy interception of a beech forest in Northern Germany. Agricultural and Forest Meteorology, 79, 131–148.

Jacobs, P., De Ceukelaire, M., De Breuck, W., & De Moor, G. (1993). Toelichtingen bij de geologische kaart van België – Vlaamse Gewest – Kaartblad Lokeren (14). Brussel: Bestuur Natuurlijke Rijkdommen en Energie & Belgische Geologische Dienst.

Jacques, D., Leterme, B., Beerten, K., Schneider, S., Finke, P., & Mallants, D. (2010). Long-term evolution of the multi-layer cover. Project near surface disposal of category A waste at Dessel. STB-NF – Version 1. NIROND-TR report 2010–03 E. Brussels: ONDRAF/NIRAS, Belgian Agency for Radioactive Waste and Enriched Fissile Materials.

Jenson, S.K., & Domingue, J.O. (1988). Extracting topographic structure from digital elevation data for Geographic Information System analysis. Photogrammetric Engineering and Remote Sensing, 54, 1593–1600.

Jongepier, I., Soens, T., Thoen, E., Van Eetvelde, V., Crombé, P., & Bats, M. (2011). The brown gold: A reappraisal of medieval peat marshes in Northern Flanders (Belgium). Water History, 3, 73–93.

Jordan, P. (2001). Ideology, material culture and Khanty ritual landscapes in western Siberia. In J.J. Fewster & M. Zvelebil (Eds.), Ethnoarchaeology and hunter-gatherers: Pictures and exhibition. BAR International Series 995 (pp. 25–42). Oxford: Archaeopress.

Kamermans, H. (2006). Problems in Paleolithic land evaluation: A cautionary tale. In M. W. Mehrer & K.L. Wescott (Eds.), GIS and archaeological site location modelling (pp. 97–122). Florida: CRC Press, Taylor & Francis.

Kasse, C., Vandenberghe, D., De Corte, F., & Van den haute, P. (2007). Late Weichselian fluvio-aeolian sands and coversands of the type locality Grubbenvorst (southern Netherlands): Sedimentary environments, climate record and age. Journal of Quaternary Science, 22, 695–708.

Kroon, T., Finke, P.A., Peereboom, I., & Beusen, A.H.W. (2001). Redesign STONE. De nieuwe schematisatie voor STONE: de ruimtelijke indeling en de toekenning van hydrologische en bodemchemische parameters. RIZA, Alterra, RIVM: Lelystad, Nederland; 99.

Mandlburger, G., Vetter, M., Milenkovic, M., & Pfeifer, N. (2011). Derivation of a countrywide river network based on airborne laser scanning DEMs—Results of a Pilot Study, 19th International Congress on Modelling and Simulation, Perth, Australia, December 12–16, 2011, pp. 2423–2429.

Navigational Map of Belgium. (2006). Kaart van de Scheepvaartwegen. NGI, 1, 25,000.

Oregon, H.A., & Fiz, I. (2008). The application of 3D reconstruction techniques in the analysis of ancient Tarraco's urban topography. In A. Posluchsny, K. Lambers, & I. Herzog (Eds.), Layers of perception. Proceedings of the 35th International Conference on Computer Applications and Quantitative Methods in Archaeology (CAA), Berlin 2007 (pp. 343–345). Bonn: KolloquienzurVor- und Frühgeschichte 10.

Price, A.G., & Carlyle-Moses, D.E. (2003). Measurement and modelling of growing-season canopy water fluxes in a mature mixed deciduous forest stand, southern Ontario, Canada. Agricultural and Forest Meteorology, 119, 69–85.

Sergant, J., Crombé, P., & Perdaen, Y. (2009). Mesolithic territories and land-use systems in north-west Belgium. In S. McCartan, R. Schulting, G. Warren, & P. Woodman (Eds.), Mesolithic Horizons. Papers presented at the Seventh International Conference on the Mesolithic in Europe, Belfast 2005 (pp. 277–281). Oxford: Oxbow Books.

Soens, T. (in press). The genesis of the Western Scheldt: Towards an anthropogenic explanation for environmental change in the medieval Flemish coastal plain (1250–1600). In E. Thoen, G. Borger, T. Soens, A. De Kraker, D. Tys, & L. Vervaet (Eds.), Landscapes or seascapes? The history of the coastal area in the North Sea region revised. Turnhout: Brepols, CORN Publication Series.

 Copyright © 2013 Wiley Periodicals, Inc.

Spikins, P. (1999). Mesolithic Northern England. Environment, population and settlement. BAR British Series 283. Oxford: Archaeopress.

Spikins, P. (2000). GIS models of past vegetation: An example from Northern England, 10,000–5000 BP. Journal of Archaeological Science, 27, 219–234.

Steenhuis, T.S., & Van Der Molen, W.H. (1986). The Thornthwaite-Mather procedure as a simple engineering method to predict recharge. Journal of Hydrology, 84, 221–229.

Terberger, T., Barton, N., & Street, M. (2006). The Late Glacial reconsidered—Recent progress and interpretations. In M. Street, N. Barton, & T. Terberger (Eds.), Humans, environment and chronology of the Late Glacial of the North European Plain. Proceedings of Workshop 14 (Commission XXXII "The Final Palaeolithic of the Great European Plain / Le paléolithique Final de la Grande PlaineEuropéenne") of the 15th U.I.S.P.P. Congress, Lisbon, September 2006 (pp. 189–207). Mainz: Verlag des Römisch-Germanischen Zentralmuseums.

Thomas, J. (1993). The politics of vision and the archaeologies of landscapes. In B. Bender (Ed.), Landscape: Politics and perspectives (pp. 1–17). Oxford: Berg.

Thornthwaite, C.W., & Mather, J.R. (1955). The water balance, publications in climatology 8/1. Centerton: Drexel Institute of Technology.

Thornthwaite, C.W., & Mather, J.R. (1957). Instructions and tables for computing potential evapotranspiration and the water balance, publications in climatology 10/3. Centerton: Drexel Institute of Technology.

Tilley, C.Y. (1994). A phenomenology of landscape: Places, paths, and monuments. Oxford: Berg.

Van Orshoven, J., Maes, J., Vereecken, H., Feyen, J., & Dudal, R. (1988). A structured database of Belgian soil profile data. Pedologie, 38, 191–206.

Van Ranst, E., & Sys, C. (2000). Eenduidige legende voor de digitale bodemkaart van Vlaanderen. Gent: Universiteit Gent.

Van Vlaenderen, J., Sergant, J., De Bock, H., & De Meireleir, M. (2006). Steentijdvondsten in de Moervaartdepressie (Oost-Vlaanderen, België). Inventaris en geografische analyse. Gent: Archeologische Inventaris Vlaanderen.

Verbruggen, C. (1971). Postglaciale landschapsgeschiedenis van zandig Vlaanderen. Botanische, ecologische en morfologische aspekten op basis van palynologisch onderzoek. Unpublished doctoral dissertation, Rijksuniversiteit Gent, Gent.

Verbruggen, C., Denys, L., & Kiden, P. (1996). Belgium. In B.E. Berglund, H.J.B. Girks, M. Ralska-Jasiewiczowa, & H.E. Wright (Eds.), Palaeoecological events during the last 15000 years: Regional syntheses of palaeoecological studies of lakes and mires in Europe. Chichester: John Wiley & Sons Ltd.

VMM. (2006). Grondwaterbeheer in Vlaanderen: het onzichtbare water doorgrond. Aalst: Vlaamse Milieumaatschappij.

VMM. (2008a). Grondwater in Vlaanderen: het Centraal Vlaams Systeem. Aalst: Vlaamse Milieumaatschappij.

VMM. (2008b). Grondwater in Vlaanderen: het Centraal Kempisch Systeem. Aalst: Vlaamse Milieumaatschappij.

Werbrouck, I., Antrop, M., Van Eetvelde, V., Stal, C., De Maeyer, P., Bats, M., Bourgeois, J., Court-Picon, M., Crombé, P., De Reu, J., De Smedt, P., Finke, P.A., Van Meirvenne, M., Verniers, J., & Zwertvaegher, A. (2011). Digital elevation model generation for historical landscape analysis based on LiDAR data, a case study in Flanders (Belgium). Expert Systems with Applications, 38, 8178–8185.

Wilsnack, M.M., Welter, D.E., Montoya, A.M., Restrepo, J.I., & Obeysekera, J. (2001). Simulating flow in regional wetlands with the MODFLOW wetlands package. Journal of the American Water Resources Association, 37(3), 655–674.

Zhang, H., & Hiscock, K.M. (2010). Modelling the impact of forest cover on groundwater resources: A case study of the Sherwood Sandstone aquifer in the East Midlands, UK. Journal of Hydrology, 392, 136–149.

Zidan, Y.O.Y. (2008). Mapping phreatic water tables to update the drainage class map 1:20,000 in the Scheldt Valley near Ghent. Unpublished masters' thesis. Ghent University, Ghent.

Zume, J.T., & Tarhule, A.A. (2011). Modelling the response of an alluvial aquifer to anthropogenic and recharge stresses in the United States Southern Great Plains. Journal of Earths System Science, 120(4), 557–572.

Zvelebil, M. (2003). Enculturation of Mesolithic landscapes. In L. Larsson, H. Kindgren, K. Knutsson, D. Leoffler, & A. Åkerlund (Eds.), Mesolithic on the Move. Papers presented at the Sixth International Conference on the Mesolithic in Europe, Stockholm 2000 (pp. 65–73). Oxford: Oxbow Books Ltd.

Zwertvaegher, A., Werbrouck, I., Finke, P.A., De Reu, J., Crombé, P., Bats, M., Antrop, M., Bourgeois, P., Court-Picon, M., De Maeyer, P., De Smedt, P., Sergant, J., Van Meirvenne, M., & Verniers, J. (2010). On the use of integrated process models to reconstruct prehistoric occupation, with examples from Sandy Flanders, Belgium. Geoarchaeology, 25, 784–814.

 Copyright © 2013 Wiley Periodicals, Inc. 